

# An optic pharyngeal manometric sensor for deglutition analysis

Shuhei Takeuchi · Haruka Tohara · Hiroyuki Kudo ·  
Kimio Otsuka · Hirokazu Saito · Hiroshi Uematsu ·  
Kohji Mitsubayashi

Published online: 30 June 2007  
© Springer Science + Business Media, LLC 2007

**Abstract** A micro optic pharyngeal manometric sensor for deglutition analysis was constructed. The optical manometric sensor was composed of a fluid-sensitive and air-sensitive fiber-optic pressure sensor (extrinsic Fabry-Perot interferometric type) and a lateral pressure-sensitive attachment. The manometric sensor was circumferential type, and had a very small diameter (distal: 2.08 mm, mesial: 0.99 mm). The output current of the sensor was linearly related to the output of a conventional catheter-type solid-state pressure sensor over a range of  $-3.0 \times 10^4$  to  $3.0 \times 10^4$  N/m<sup>2</sup>. The time constants of responsiveness were  $12.2 \pm 2.7$  ms during rapid decompression and  $32.1 \pm 1.6$  ms after a rapid return to ambient pressure. The optical pharyngeal manometric sensor had similar response time characteristics as the naked optical sensor and the conventional solid-state sensor. During *in vivo* measurement, the waveform of the optical pharyngeal manometer output was almost similar to the waveform of the output of the conventional sensor. The optical manometer could sufficiently detect the lateral pressure and the suction pressure for bolus transit generated in the P–E segment.

**Keywords** Fiber-optic pressure sensor · Pharyngeal manometry · Fabry–Perot interferometer · Swallowing disorder · Oropharyngeal dysphagia

## 1 Introduction

Oropharyngeal dysphagia is common in the elderly (Sheth and Diner 1988; Lindgren and Janzon 1991; Dejaeger et al. 1994). The causes of oropharyngeal dysphagia are multiple and include neurologic, myopathic, structural, infectious, metabolic, and iatrogenic disorders. A decline of deglutition function frequently produces aspiration pneumonia, and it induces significant morbidity, mortality, and costs (Bammer et al. 2002). Pneumonia is often fatal to elderly people. In addition, deglutition functional decline is caused by pathological aging as well as by physiological aging. Therefore, the routine examination of the swallowing function of aged patients is meaningful of a vital prognosis. Recently, pharyngeal manometers have been used in some medical facilities for the evaluation of swallowing function.

The pharyngeal manometer is one of the diagnosis approaches of deglutition function. Until now, pharyngeal manometer systems have been perfusion catheter systems with strain gauges (Dodds et al. 1975; Lydon et al. 1975; Cook et al. 1989) and the catheter type solid-state sensor systems. Most research studies over the past few years have used the latter system because it is more sensitive to the rapid timing and pressure changes of the pharynx in comparison to the perfusion catheter system. So the solid-state sensor systems have been currently used in medical use. However, many previous catheters had thick diameters, for example, o.d. 2.5 mm (Kahrilas et al. 1992), o.d. 4.6 mm (Bülow et al. 2002) and o.d. 5 mm (Dejaeger et al. 1997). The diameter of the catheter should be as small as

---

S. Takeuchi · H. Tohara · H. Uematsu  
Department of Gerodontology,  
Division of Gerontology and Gerodontology, Graduate School,  
Tokyo Medical and Dental University,  
1-5-45 Yushima, Bunkyo-ku,  
Tokyo 113-8510, Japan

H. Kudo · K. Otsuka · H. Saito · K. Mitsubayashi (✉)  
Department of Biomedical Devices and Instrumentation,  
Institute of Biomaterials and Bioengineering  
Tokyo Medical and Dental University,  
2-3-10 Kanda-Surugadai, Chiyoda-ku,  
Tokyo 101-0062, Japan  
e-mail: m.bdi@tmd.ac.jp

possible because nasal and pharyngeal discomforts increase significantly with increase in diameter (Salassa et al. 1998). In addition, it is reported that as patient discomforts and catheter diameter increase, various pressures generated in the pharynx increase in normal subjects (Cook et al. 1989). Such discomforts make the conventional pharyngeal manometer unacceptable to patients and prevent pharyngeal manometry from being performed correctly. A smaller sensor diameter is a very important factor in order to not feel discomfort for dyphasic children and patients with nasal diseases that tend to have a narrow inferior meatus. There was a thin diameter sensor (o.d. 2.1 mm (Hiss and Huckabee 2005)), but it was a unilateral type solid-state sensor. Sensors for pharyngeal manometry are inserted from the nasal route, and reached the upper esophagus via the pharynx. Therefore it is difficult to control the direction of the pressure sensitive region when using unilateral type sensors.

The objective of this study was to construct an acceptable and circumferential optical fiber based pharyngeal manometric sensor with for analyzing the deglutition mechanism and to use it to perform *in vivo* measurements. The minimum diameter of a circumferential solid-state sensor used as a pharyngeal manometer has been reported to be 2.2 mm. The use of an optical fiber device enables such pharyngeal manometer to become thinner and more flexible. In addition, by using a pressure sensitive attachment, the structure of the sensor as a pharyngeal manometer can be simplified and it is also easy to produce.

## 2 Experimental section

### 2.1 Construction of an optic pharyngeal manometric sensor

A circumferential-type optical pressure sensor for measuring various pharyngeal pressures was constructed. This sensor was composed of a fluid- and air-sensitive fiber-optic pressure sensor (FOP-MIV, FISO Technologies Inc. Quebec, PC, Canada) and pressure-sensitive attachment at the tip of the sensor. The naked optical sensor without the attachment had an o.d. 0.99 mm. The attachment was made up of a thin PTFE tube (the wall thickness = 0.051 mm), a styrene stick, a silicone sealing tube, and physiological saline. Therefore, the distal diameter was 2.08 mm and the mesial diameter was 0.99 mm (Fig. 1). The length of pressure-sensitive part of the PTFE tube was 15 mm, which was based on the average width of the presser zone of the upper esophageal sphincter (Fukuzumi et al. 1987). The styrene stick easily facilitated the insertion of the sensor into the pharynx. The role of the physiological saline, which is an incompressible fluid, was to transmit the pressure to the diaphragm. Consequently, the pressure from any direction in the P–E segment can be detected.

The pressure transmitted to the diaphragm was measured by the extrinsic Fabry–Perot interferometric (EFPI) technique (Murphy et al. 1991; Kaufman et al. 2003). EFPI technology is a distance measurement technique based on the formation of a low-finesse Fabry–Perot cavity between the polished end of a fiber and a reflective surface, which is the undersurface of a diaphragm. It utilizes that the absolute air gap information is contained in the frequency content of the signal (Murphy et al. 1991; Wavering et al. 2000).

### 2.2 Performance evaluation of the sensors

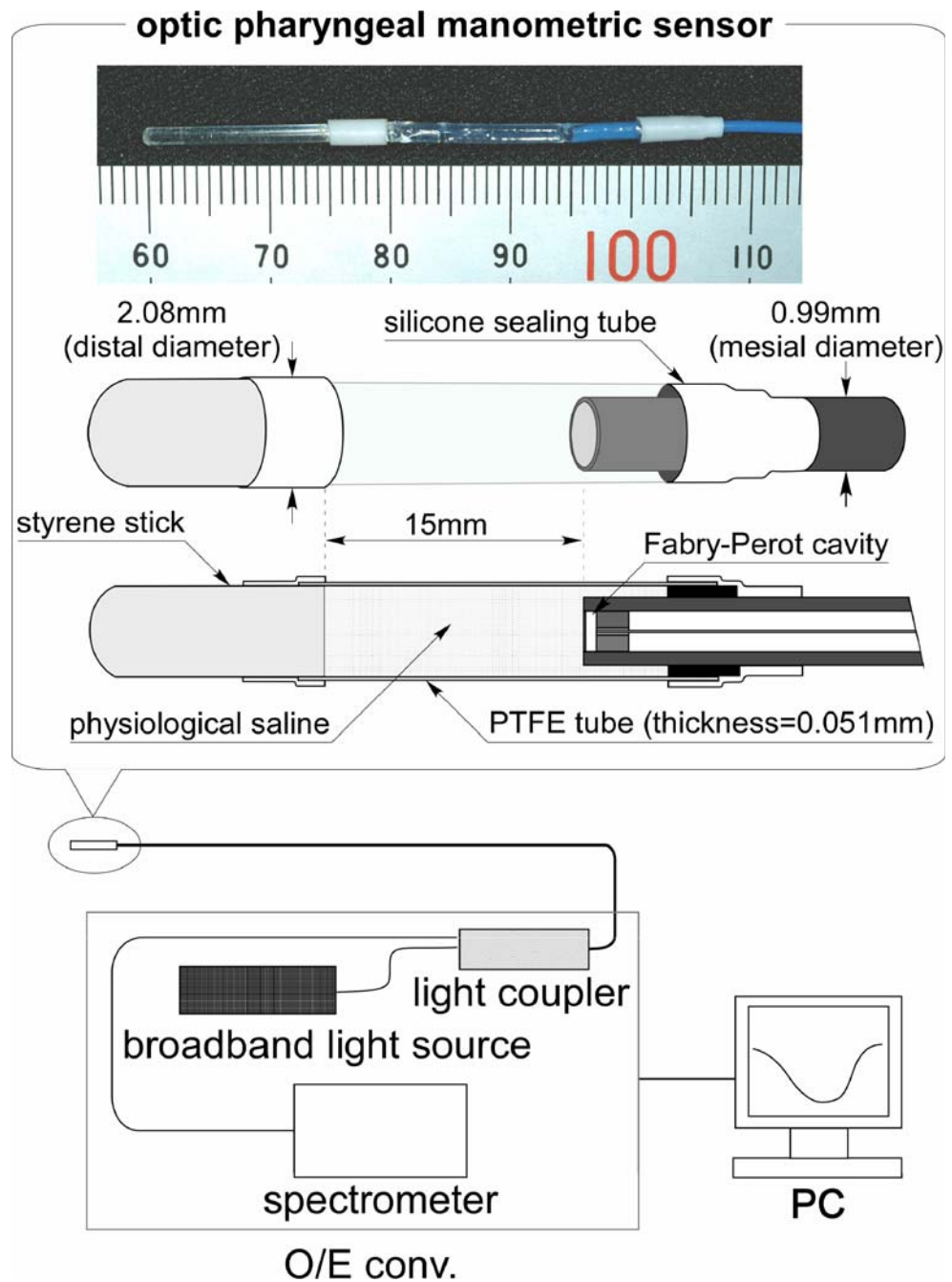
#### A. Evaluation of static characteristics

In this test, the closed space was slowly pressurized from  $-3.0 \times 10^4$  to  $3.0 \times 10^4$  N/m<sup>2</sup> by a syringe pump with a flow controller for 180 s (Fig. 2). The output of the optic pharyngeal manometric sensor was compared to the output of a synchronized catheter-type solid-state pressure sensor (P37-4109C05, Zinetics Inc. Salt Lake City, UT, USA). This solid-state sensor is shown in Fig. 3. It is commercially available and has been widely used in medical use. The catheter (o.d. 3.90 mm) has four microtransducers. The distal sensor is the circumferential transducer. It consists of a silastic annulus enclosing a small transducer within a castor oil-filled chamber. The other three sensors are unilateral, and the sensitive directions of each sensor are rotated every 120°. The characteristics of the conventional sensor showed 2.6% accuracy and 0.13% linearity. In this study the far medial sensor that is clinically sat in the important position was compared to the optical sensor. This experiment was repeated five times and linear regression lines were determined during static characterization pressure ramps.

#### B. Dynamic response behavior

The dynamic response of the sensors was examined using two methods. In the first method, the depressurized space ( $-2.0 \times 10^4$  N/m<sup>2</sup>) was created by a suction pump (B-1), and a pressure valve was subsequently opened rapidly (Fig. 2). The fast pressure increase of the sensors was recorded. This test was repeated five times, and the time constants as responsiveness were evaluated. The time constants represent the time required to reach about 63.2% of its final value from the moment of opening the pressure valve. The second test used a balloon. The pressurized space ( $2.0 \times 10^4$  N/m<sup>2</sup>) was made in a balloon (B-2). The balloon bursting with fire was used to make a sharp pressure decrease (Fig. 2), because it can prevent the oscillation of the signal at initial response (Yang et al. 1978). The time constants were also evaluated in this test.

**Fig. 1** Schematic diagram of the optic pharyngeal manometric sensor with saline inside a thin PTFE tube for pressure transmission



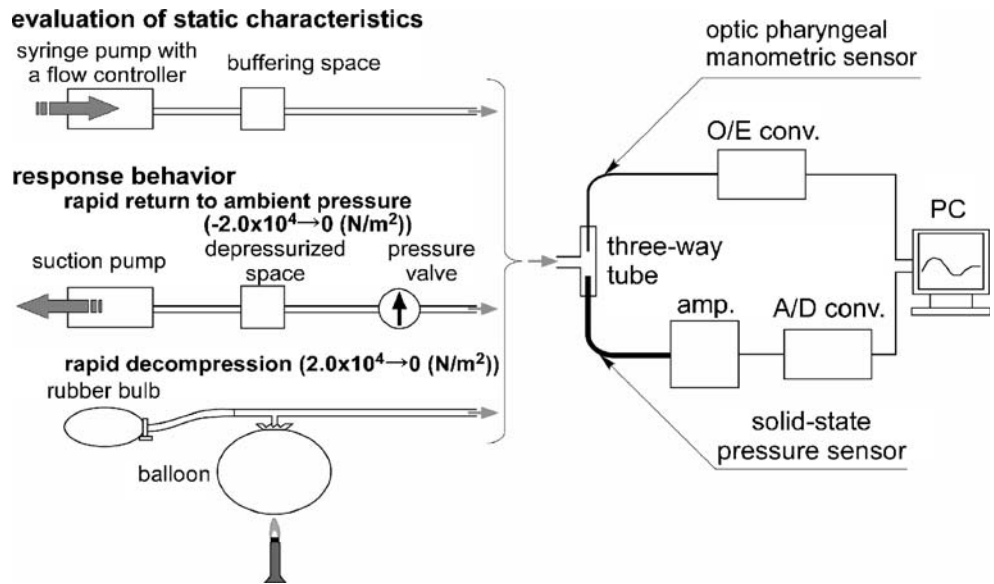
### 2.3 Pharyngeal manometry

In the pharyngeal manometry, the pressure generated in the pharyngeal esophageal segment (P–E segment) has great importance. This is because that the P–E segment is close to the entrance of the trachea, so a dysfunction in the P–E segment is directly linked to aspiration. We therefore measured the pressure, focusing our attention on the P–E segment.

*In vivo* measurement was performed on one subject, a man in his 20s. He had no symptoms of oropharyngeal or upper gastrointestinal dysfunction. Informed consent

was obtained after the benefits and possible adverse effects of the examination had been fully explained to the subject. The subject sat on a chair with a backrest, and the head and the axial plane of the body were aligned in a straight line. Also, the head of the subject was positioned in a normal upright swallowing position in front of an endoscope and the optic pharyngeal manometer screen. The optic pharyngeal manometric sensor and the conventional catheter type solid-state pressure sensor were inserted into the pharynx at the same time while monitoring with an endoscope (Fig. 4). Both sensors were inserted through the nasal route,

**Fig. 2** Experimental set-up for the evaluation of sensors characteristics



which enables the measurement of swallowing pressures in the pharynx without being inhibited by tongue motion and mastication (McConnell et al. 1988a). The detection component of the PTFE tube attachment at the optical manometer was set beside the far medial sensor of the solid-state sensor. The sensors were placed in the P–E segment of the hypopharynx. After the subject’s breathing was stable, three dry swallows were performed every 5 s after a command given by the tester. The signals from both sensors were recorded simultaneously.

**3 Results and discussion**

**3.1 Evaluation of static characteristics**

The pressure of the optic pharyngeal manometric sensor ( $P_o$ ) was linearly related to the pressure of the solid-state pressure sensor ( $P_s$ ) over a range of  $-3.0 \times 10^4$  to  $3.0 \times 10^4$  N/m<sup>2</sup>

(Fig. 5), with a correlation coefficient of 0.999 deduced by a regression analysis. The value was by the following equation:

$$P_o \text{ (N/m}^2\text{)} = -338.8 + 1.0965 [P_s \text{ (N/m}^2\text{)}]$$

In addition, the regression lines of the five tests converged into about 0.3% of the full-scale output. As a result, the optical manometric sensor had relatively sufficient stable and accurate output, considering that the solid-state sensor had 2.6% accuracy and 0.13% linearity. Also, it found that this optical manometer had acceptable static characteristics over the swallowing pressure range of  $-0.5 \times 10^4$  to  $3.0 \times 10^4$  N/m<sup>2</sup>.

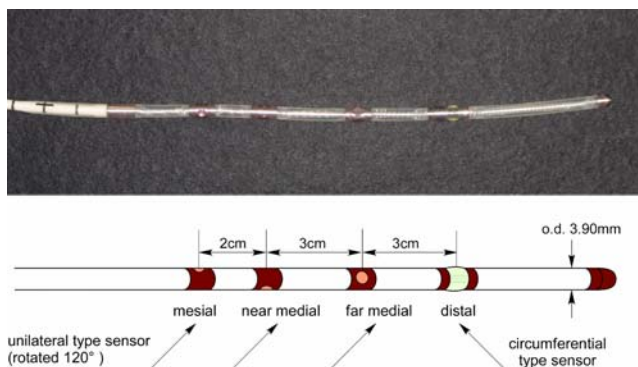


**Fig. 3** Diagram of the catheter-type solid-state pressure sensor

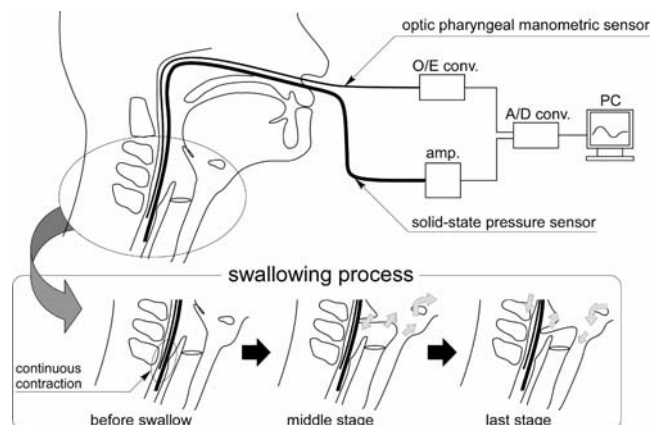


**Fig. 4** Pharyngeal manometric measurement. The changes of the various pharyngeal pressures in the P–E segment generated by the surrounding muscles during three dry swallows were recorded



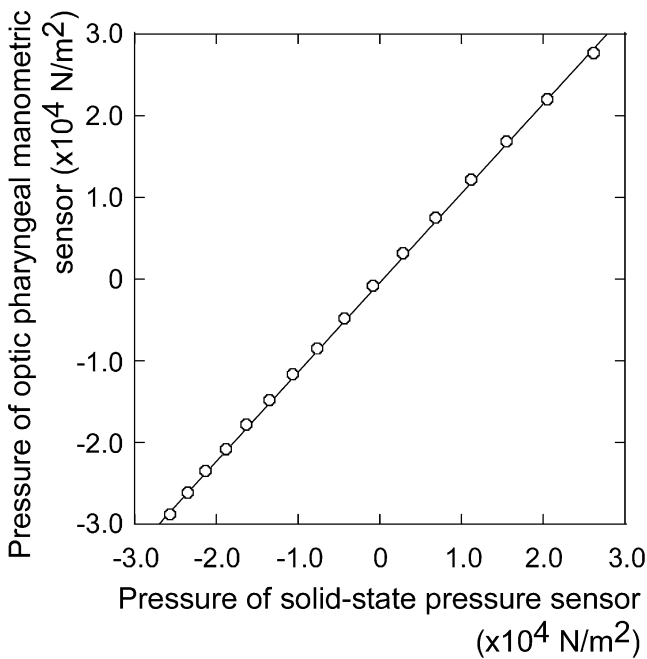


**Fig. 5** Relationship between the pressure of the optic pharyngeal manometric sensor and the pressure of the conventional solid-state sensor in the pressurized space at the constant. The sampling rate was 10 Hz. The values were plotted for every 100 samples

### 3.2 Evaluation of the responsiveness of the optical pressure sensor

The outputs of the three types of pressure sensors during rapid pressure changes are shown in Fig. 6, and calculated time constants are presented in Table 1. During the rapid decompression evaluation, the sensors displayed a better response time in comparison to the response during the rapid return to ambient pressure. This was because of using fire, not a needle, at the balloon bursting. This method could prevent the oscillation of the signal at the initial response, and provide an instantaneous pressure change. So balloon bursting with fire is considered to be an effective method for evaluating the sensor response functions accurately and easily.

At both experiences, the optical pharyngeal manometric sensor showed a slight delay in comparison to the other sensors. It is expected that the responsiveness of the optic pharyngeal manometer can be improved by improving coupling to the Fabry Perot sensor region attachment.

### 3.3 Deglutition analysis with the optic pharyngeal manometer

The conventional solid-state sensor and the optical pharyngeal manometric sensor were simultaneously used during *In vivo* measurement. The optical sensor was o.d. 2.08 mm in the P–E segment, on the other hand in the inferior meatus,

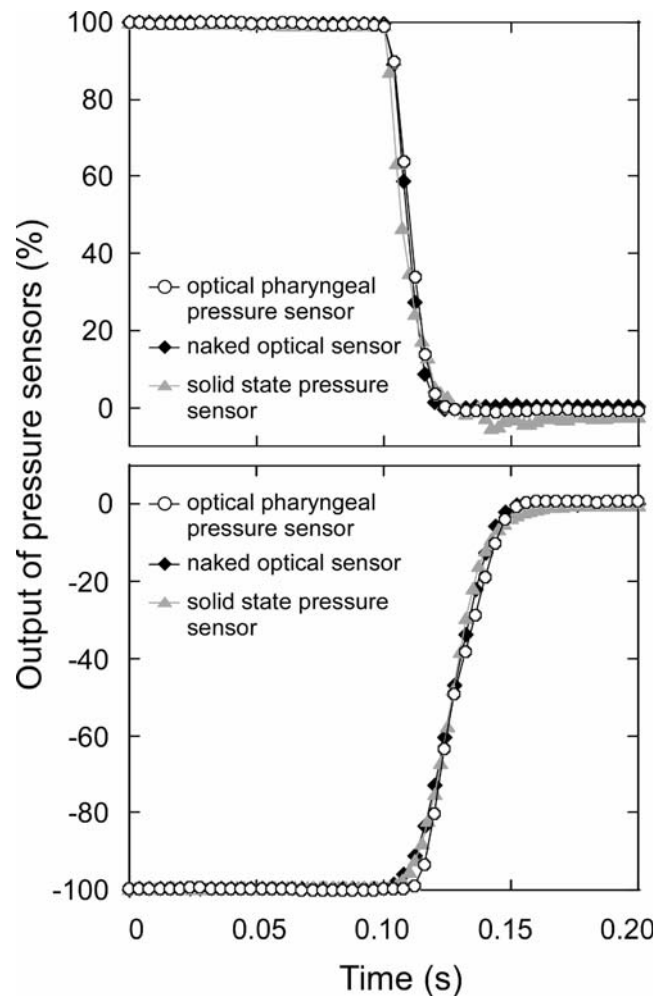


**Fig. 6** Dynamic response of pressure sensors. The upper figure is the graph of the response to rapid decompression. The lower figure shows a graph of the response to a rapid return to atmosphere. The three-point calibration ( $0, \pm 2.0 \times 10^4 \text{ N/m}^2$ ) was performed using a manometer, and  $\pm 100\%$  means  $\pm 2.0 \times 10^4 \text{ N/m}^2$ , respectively. The sampling rate of the optical pharyngeal pressure sensor and the naked optical sensor were 250 Hz, and that of the solid-state pressure sensor was 400 Hz

the sensor diameter was 0.99 mm. Therefore it was easy to insert into the pharynx from the nostril, and discomfort that a subject felt was little.

Signals of the pharyngeal manometry series of three dry swallows in the P–E segment are shown in the upper part of

**Table 1** Time constants of pressure sensors

Sensor type	Mean $\pm$ S.D. (ms) ( $n=5$ )	
	Rapid decompression	Rapid return to atmosphere
Optic pharyngeal manometric sensor	12.2 $\pm$ 2.7	32.1 $\pm$ 1.6
Naked optical sensor	11.5 $\pm$ 1.2	30.2 $\pm$ 4.3
Solid-state pressure sensor	10.6 $\pm$ 2.1	30.0 $\pm$ 4.7

Fig. 7. The enlarged figure during first swallow is shown in the lower part of Fig. 7. The overall waveforms of the optic pharyngeal manometric sensor output and the conventional solid-state pressure sensor output were almost similar. And the optical pharyngeal sensor curves are smoother than those of the solid-state sensor. This is because of the difference in the direction of pressure-sensitive region at both sensors.

In the upper figure, the sensors recorded a static lateral pressure which was defined as the resting pressure generated in the P–E segment by the continuous contraction of cricopharyngeal muscle. It has important roles as an anti-reflux barrier and as a barrier to entrance of air into the esophagus during inspiration (Miller et al. 2004). The optic pharyngeal manometer could record about  $6.5 \times 10^3 \text{ N/m}^2$  as the resting pressure. On the other hand the conventional sensor sensed about  $8.7 \times 10^3 \text{ N/m}^2$  as the resting pressure. This difference is due to the difference in the diameter of the sensors, and an increased diameter resulted in an increase in the value of the resting pressure.

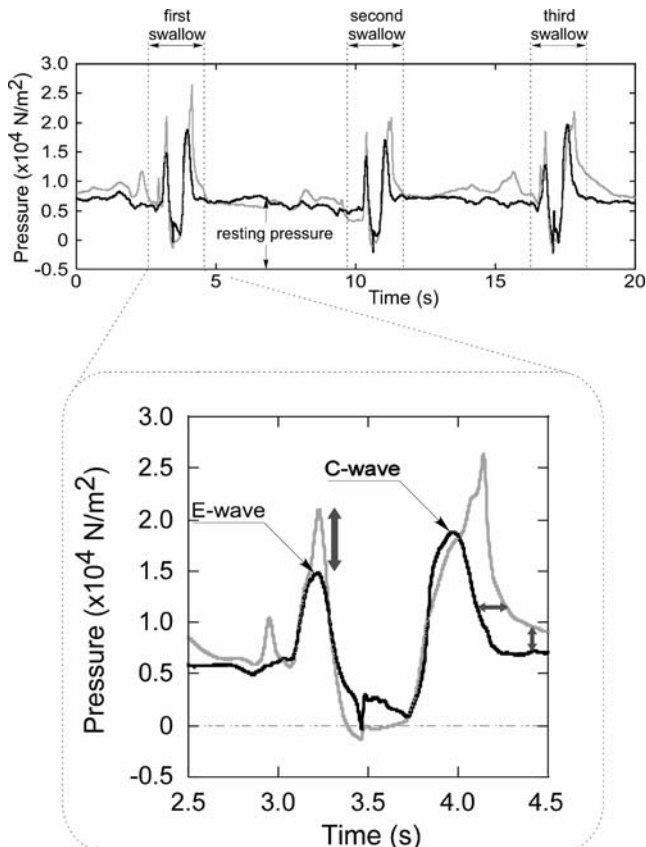


**Fig. 7** Outputs of the optic pharyngeal manometer and the conventional solid-state sensor *in vivo*. The gray line and the black line represent the conventional sensor and the optical manometer, respectively. In the enlarged figure, broad arrows showed influence of difference of both sensor diameters

In the lower figure, there were two positive curves and one negative curve (“M”-shaped configuration (Castell et al. 1990)) during a swallow. The M-shaped configuration appeared during swallow when pharyngeal manometric sensors were correctly recorded in the P–E segment.

The first positive curve is a dynamic lateral pressure, which is called an elevation pressure wave (*E*-wave). The *E*-wave is superimposed on the resting pressure and is related to the elevation of the laryngopharynx. The negative curve represents the suction pressure in the P–E segment. The negative pressure is generated by a laryngeal elevation and it has been reported to be one of important factors in bolus transit (McConnell 1988b). In the lower figure the suction pressure that was below the zero-line shown an output of about  $-2.2 \times 10^3 \text{ N/m}^2$  at the minimum. The second positive curve is also a dynamic lateral pressure, and termed the constrictor wave (*C*-wave). The *C*-wave is generated by a series of pharyngeal posterior wall contractions and laryngeal shortening. This pressure is applied onto the tail of the bolus and is considered to be a bolus-clearing pressure.

At any point on the *E*-wave, the negative pressure and the *C*-wave of the optic pharyngeal manometer were different from those of the conventional sensor regarding the pressure value and the timing at the peak. The reasons for this effect include the differences in the diameter of the sensors and the low elasticity of the PTFE tube affecting response to the dynamic pressure changes. If using only the optical pharyngeal manometer, it is possible to obtain signals that resemble those from the solid-state sensor. And by making an attachment with more elasticity, the sensor will respond better to a dynamic pressure change.

#### 4 Conclusions

A micro-optical pharyngeal manometric sensor for deglutition analysis was constructed in this study. This sensor was a circumferential type which is easy to produce. The distal diameter of the optical manometric sensor was 2.08 mm in the P–E segment, and mesial diameter was 0.99 mm in the inferior meatus. The sensor is thinner than other circumferential type sensors currently in use.

The pressure of the optical fiber-based pharyngeal manometric sensor was linearly related to the pressure of a conventional catheter-type solid-state pressure sensor over a range of  $-3.0 \times 10^4$  to  $3.0 \times 10^4 \text{ N/m}^2$ . The time constants of the sensor were  $12.2 \pm 2.7 \text{ ms}$  during a rapid decompression and  $32.1 \pm 1.6 \text{ ms}$  at a rapid return to ambient pressure. It was found that this sensor had characteristics similar to a naked optical sensor and the conventional solid-state sensor.

In the pharyngeal manometry, the optic pharyngeal manometric sensor could accurately record the lateral pressure and the suction pressure in the P–E segment. The waveform of the optical manometer was closely similar to that of the conventional sensor, although the findings were influenced by the difference in the diameters of the sensors and the elasticity of the PTFE-tube of the attachment.

Future work should be undertaken to modify the attachment in order to improve the response to dynamic pressure change. In addition, it would be useful to develop a new clinical instrument that unifies an endoscope and the optic pharyngeal manometer. This instrument could be used for the new rehabilitation of patients with swallowing disorders.

**Acknowledgement** This research was supported by the Research Grant for Longevity Sciences (H16-1) from the Ministry of Health, Labour and Welfare, Japan.

## References

- T. Bammer, J.R. Salassa, P.J. Klingler, *Otolaryngol. Head Neck Surg.* **127**(4), 299–308 (2002)
- M. Bülow, R. Olsson, O. Ekberg, *Dysphagia* **17**, 197–201 (2002)
- J.A. Castell, C.B. Dalton, D.O. Castell, *Am. J. Physiol.* **258**, G173–G178 (1990)
- I.J. Cook, J. Dent, S.M. Collins, *Dig. Dis. Sci.* **34**(5), 672–676 (1989)
- E. Dejaeger, W. Plemans, G. Bibau, E. Ponette, *Dysphagia* **9**(3), 156–161 (1994)
- E. Dejaeger, W. Plemans, E. Ponette, E. Joosten, *Dysphagia* **12**(2), 63–67 (1997)
- W.J. Dodds, W.J. Hogan, S.B. Lydon, E.T. Stewart, J.J. Steff, R.C. Arndorfer, *J. Appl. Physiol.* **39**(4), 692–696 (1975)
- T. Fukuzumi, D. Jinnai, K. Naveya, T. Kakegawa, *Surgery of the Esophagus* (Kanehara & Co., Ltd, Tokyo, 1987), chap. 2(4), pp. 45–46
- S.G. Hiss, M.L. Huckabee, *Dysphagia* **20**(2), 149–156 (2005)
- P.J. Kahrilas, J.A. Logemann, S. Lin, G.A. Ergun, *Gastroenterology* **103**(1), 128–136 (1992)
- K.R. Kaufman, T. Wavering, D. Morrow, J. Davis, R.L. Lieber, J. *Biomech.* **36**(2), 283–287 (2003)
- S. Lindgren, L. Janzon, *Dysphagia* **6**(4), 187–192 (1991)
- S.B. Lydon, W.J. Dodds, W.J. Hogan, R.C. Arndorfer, *Am. J. Dig. Dis.* **20**(10), 968–970 (1975)
- F.M. McConnell, D. Cerenko, R.T. Jackson, T.N. Guffin Jr., *Arch. Otolaryngol. Head Neck Surg.* **114**(12), 1413–1418 (1988a)
- F.M. McConnell, *Laryngoscope* **98**(1), 71–78 (1988b)
- L.S. Miller, Q. Dai, B.A. Sweitzer, V. Thangada, J.K. Kim, B. Thomas, H. Parkman, A.M. Soliman, *Dig. Dis. Sci.* **49**(5), 703–709 (2004)
- K.A. Murphy, M.F. Gunter, A.M. Vengsarkar, R.O. Claus, *Opt. Lett.* **16**(4), 273–275 (1991)
- J.R. Salassa, K.R. Devault, F.M. McConnell, *Dysphagia*, **13**(2), 105–110 (1998)
- N. Sheth, W. Diner, *Dysphagia* **2**(4), 209–215 (1988)
- T. Wavering, S. Meller, M. Evans, C. Pennington, M. Jones, R.V. Tassel, K.A. Murphy, W. Velander, E. Valdes, in *SPIE Biochemical and Biomolecular Sensing*, Boston, MA, 5–8 November 2000, pp. 10–16
- S.S. Yang, L.G. Bentivoglio, V. Maranhao, H. Goldberg, *Basic Measurement and Calculations*, in *Cardiac Catheterization Data to Hemodynamic Parameters Basic* (F.A. Davis Co, Philadelphia, 1978), pp. 24–27